SPECTRAL CLASSIFICATION AND UNMIXING WITH MICROIMAGING SPECTROSCOPY OF MAFIC ROCK CORES FROM THE OMAN DRILLING PROJECT: IMPLICATIONS FOR PLANETARY DATASET ANALYSIS. R. N. Greenberger[1], B. L. Ehlmann[1,2], P. B. Kelemen[3], C. E. Manning[4], M. Harris[5], D. A. H. Teagle[6], and the Oman Drilling Project Phase 1 Science Party, [1]Div. of Geological and Planetary Sciences, California Institute of Technology, 1200 E. California Blvd., Pasadena, CA 91125 (rgreenbe@caltech.edu), [2]Jet Propulsion Laboratory, California Institute of Technology, Pasadena, CA. [3]Columbia University, Palisades, NY. [4]University of California Los Angeles, Los Angeles, CA. [5]Plymouth University, Plymouth, UK. [6]University of Southampton, Southampton, UK.

Introduction: Remote infrared spectroscopy is the primary tool for determination of surface compositions on planetary bodies [e.g., 1–4]. Characteristic absorption features are dependent on chemistry and structure and are used to pinpoint mineral, ice, and organic components [e.g., 5,6]. With imaging spectroscopy, spatially-resolved reflectance of light is measured simultaneously at many contiguous wavelengths [7]. Meters-scale/pixel or greater spatial resolution is most commonly employed for orbital and airborne instruments, but application for earth and planetary sciences at sub-mm to cm scale in the laboratory and field is a newly emerging tool [8]. In addition to providing new insights into geologic processes through sub-mm mineral mapping, microscale measurements also validate and improve coarser resolution orbital observation analysis.

A critical, ongoing challenge in interpretation of visible-shortwave infrared (VSWIR) spectroscopic datasets is determining the best method of identification and quantification of mineral components within single pixels. Classification algorithms identify the spectrally dominant component(s) within each spectrum but not their abundance [e.g., 9–11]. Linear [e.g., 12] and non-linear [e.g., 13,14] unmixing methods produce abundances with varying degrees of success depending on the phases present, the spatial scale of mixing, and the precise algorithm. Tests of these algorithms with natural, non-particulate rock surfaces, as are present in rock outcrops on planetary surfaces, are limited in part because of the difficulty in coordinating reflectance spectra with mineralogy determined through other laboratory techniques within individual pixels [15–17].

Here, we use a unique dataset, imaging spectroscopy of the Oman Drilling Project mafic, ultramafic, and metamorphic drill cores, encompassing a wider range of minerals and grain sizes/textures than most previous studies, to test spectral classification and unmixing algorithms. The results will illuminate where existing methods succeed, where they struggle, and where future work is needed to improve interpretations of these datasets.

Methods: VSWIR reflectance spectra were measured of the full 1.5-km of the Oman Drilling Project Phase 1 drill cores aboard the Japanese drilling vessel Chikyu at 250-260 μm/pixel with the Caltech imaging

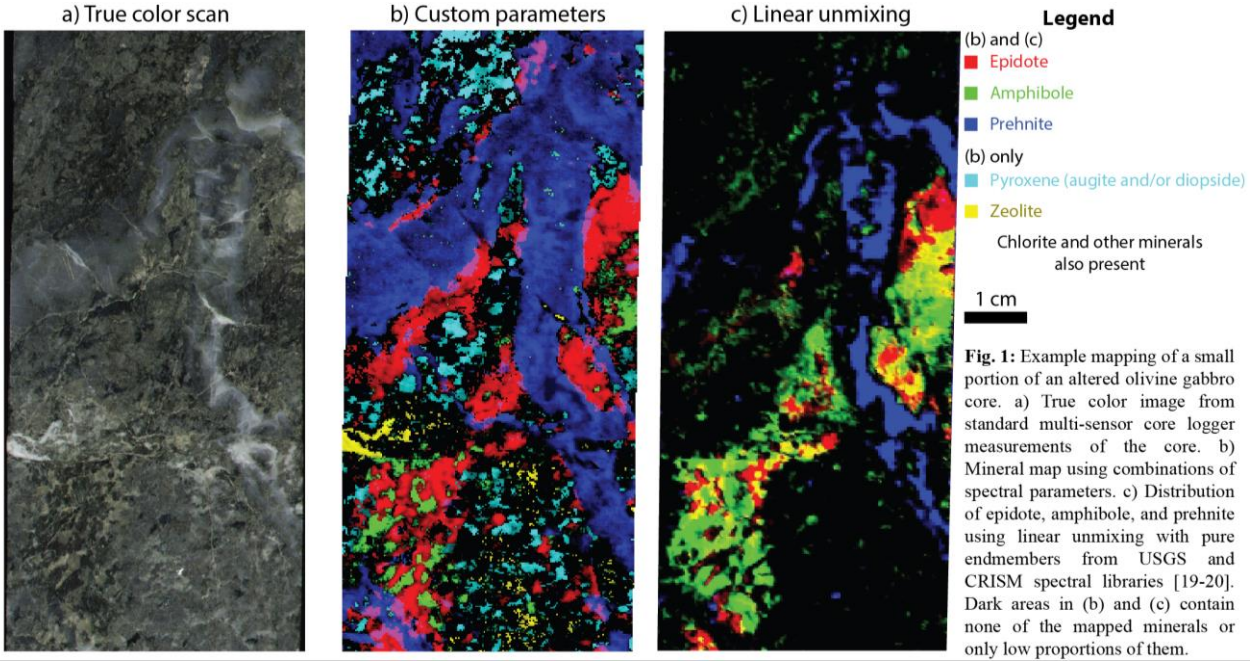

Fig. 1: Example mapping of a small portion of an altered olivine gabbro core. a) True color image from standard multi-sensor core logger measurements of the core. b) Mineral map using combinations of spectral parameters. c) Distribution of epidote, amphibole, and prehnite using linear unmixing with pure endmembers from USGS and CRISM spectral libraries [19-20]. Dark areas in (b) and (c) contain none of the mapped minerals or only low proportions of them.

spectrometer, comprising nearly 14 TB of raw data (e.g., Fig. 1). These cores, from the Samail ophiolite, Oman, are of oceanic crust, including gabbros and sheeted dikes, listvenite (carbonate, quartz), and the underlying metamorphic thrust. Portions of the gabbros and sheeted dikes have undergone hydrothermal alteration. These cores contain a large proportion of the mineral diversity identified thus far on Mars and some asteroids [1,18,19].

The imaging spectrometer system, custom built for Caltech by Headwall Photonics, contains visible-near infrared (VNIR) and shortwave infrared (SWIR) sensors co-boresighted and mounted on an optical bench. The wavelength range is 0.4-2.6 μm with 5 nm (VNIR) and 6 nm spectral resolution (SWIR). Core was moved below the instrument on the Chikyu's multi-sensor core logger track. The core and a Spectralon calibration target were illuminated with a halogen slit lamp, and measurements were corrected for dark current and the absolute reflectance properties of Spectralon.

So far, minerals have been mapped using combinations [e.g., 15] of individual spectral parameters [9–11] that indicate the presence and absence of key absorption features diagnostic of minerals and basic linear unmixing using endmembers from the USGS and CRISM spectral libraries [19,20]. We will also present results of analyses using methods such as spectral feature fitting, mixture-tuned matched filtering, CRISM spectral parameters [10,11], and Tetracorder [17]. We will explore non-linear unmixing algorithms [e.g., 13,14], though the nearly 28 TB (processed) size of the full dataset may preclude application of such complex algorithms for mapping all core intervals. For this presentation, we focus image analyses on ten samples from these cores, which will also be analyzed with SEM to validate the spectral signatures, and core intervals with XRD measurements from the Oman Drilling Project Phase 1 core description for validation.

Results: Manual inspection of spectra and parameter mapping identify high-Ca pyroxene (augite and/or diopside) along with many secondary minerals, including phyllosilicates, zeolites, prehnite, epidote, amphibole, and gypsum, and carbonate. The listvenite contains Mg-, Mg/Ca-, and Ca-bearing carbonates, quartz, iron oxides, serpentine, and more. The parameters used thus far (Fig. 1b) work well, though there are challenges distinguishing minerals with multiple overlapping absorption features, particularly when two or more of these minerals are closely intergrown. Linear unmixing may identify more mixing than the spectral parameters but does not detect certain large areas with absorption features characteristic of minerals such as prehnite (Fig. 1c), possibly due to overlapping absorption features of several minerals (especially chlorite) present in the 2.30-2.35 μm range that are likely intergrown with the prehnite. This result may also be due to non-optimal endmember and wavelength selection for linear unmixing, which will be investigated further. We will also determine whether other mapping methods are more accurate.

Critical petrologic information as to the time ordering of alteration can be gleaned using these mineral maps. For example, in Fig. 1, a prehnite-bearing vein (blue) crosscuts epidote (red), and a zeolite vein (yellow, Fig. 1b) crosscuts prehnite. Similar analyses have been completed previously with micro-imaging spectroscopy of meteorites [8,21,22] and planetary analog samples [8,15,16]. This technique presents advantages over traditional measurements of single points or powdered samples, such as XRD, where only a small number of points can be analyzed and/or the petrographic context is lost during sample preparation.

Implications: The results of laboratory tests of micro-imaging spectroscopy, combined with validation with other measurements, scale to lander- and orbiter-based imaging spectroscopy observations of planetary surfaces and improve our capabilities. Here, parameters are successfully used for the identification of the presence of minerals of interest, and we will present results comparing commonly used algorithms and their accuracy and discuss the implications for methods of analysis of planetary remote sensing datasets. In addition, imaging spectrometers would provide invaluable contextual mineralogic information on a future landed mission, but the large data volumes require onboard data processing algorithms to downlink derived data products [23]. Laboratory micro-imaging spectroscopy studies will lead to improvements in these algorithms.

References: [1] Bibring J.-P. et al. (2006) *Science* **312**, 400–404. [2] Mustard J. F. et al. (2008) *Nature* **454**, 305–309. [3] Pieters C. M. et al. (2009) *Science* **326**, 568–572. [4] McCord T. B. et al. (1998) *Science* **280**, 1242–1245. [5] Hunt G. R. and Ashley R. P. (1979) *Econ. Geol.* **74**, 1613–1629. [6] Clark R. N. et al. (1990) *JGR* **95**, 12653–12680. [7] Goetz A. F. H. et al. (1985) *Science* **228**, 1147–1153. [8] Greenberger R. N. et al. (2015) *GSA Today* **25**, 4–10. [9] Clark R. N. and Roush T. L. (1984) *JGR* **89**, PP. 6329-6340. [10] Pelkey S. M. et al. (2007) *JGR* **112**, 18 PP. [11] Viviano-Beck C. E. et al. (2014) *JGR* **119**, 1403–1431. [12] Adams J. B. et al. (1986) *JGR* **91**, 8098–8112. [13] Hapke B. (1981) *JGR* **86**, PP. 3039-3054. [14] Shkuratov Y. et al. (1999) *Icarus* **137**, 235–246. [15] Greenberger R. N. et al. (2015) *GCA* **171**, 174–200. [16] Leask E. K. and Ehlmann B. L. (2016) *IEEE WHISPERS*, 1-5. [17] Clark R. N. et al. (2003) *JGR* **108**. [18] Ehlmann B. L. and Edwards C. S. (2014) *Annu. Rev. Earth Planet. Sci.* **42**, 291–315. [19] Murchie S. L. et al. (2009) *JGR* **114**, 30 PP. [20] Clark R. N. et al. (2007) *USGS Digital Spectral Library Splib06a: USGS, Data Series 231*. [21] Green R. O. et al. (2015) *46th LPSC*, Abstract# 2154. [22] Fraeman A. A. et al. (2016) *IEEE WHISPERS*, 1–5. [23] Ehlmann B. L. et al. (2014) *45th LPSC*, Abstract# 2824.

Acknowledgments: We would like to thank the Oman Drilling Project Phase 1 core description teams, whose numerous analyses and descriptions provide the validation for this portion of our study.